



CAN UNCLASSIFIED



DRDC | RDDC
technologysciencetechnologie

Target localization over the Earth's curved surface

S. Wong,
R. Jassemi-Zargani
D. Brookes
B. Kim
DRDC – Ottawa Research Centre

B. Kaluzny
DRDC – Centre for Operational Research and Analysis

Defence Research and Development Canada

Scientific Report

DRDC-RDDC-2018-R136

May 2018

CAN UNCLASSIFIED

CAN UNCLASSIFIED

IMPORTANT INFORMATIVE STATEMENTS

This document was reviewed for Controlled Goods by Defence Research and Development Canada (DRDC) using the Schedule to the *Defence Production Act*.

Disclaimer: Her Majesty the Queen in right of Canada, as represented by the Minister of National Defence ("Canada"), makes no representations or warranties, express or implied, of any kind whatsoever, and assumes no liability for the accuracy, reliability, completeness, currency or usefulness of any information, product, process or material included in this document. Nothing in this document should be interpreted as an endorsement for the specific use of any tool, technique or process examined in it. Any reliance on, or use of, any information, product, process or material included in this document is at the sole risk of the person so using it or relying on it. Canada does not assume any liability in respect of any damages or losses arising out of or in connection with the use of, or reliance on, any information, product, process or material included in this document.

Endorsement statement: This publication has been peer-reviewed and published by the Editorial Office of Defence Research and Development Canada, an agency of the Department of National Defence of Canada. Inquiries can be sent to: Publications.DRDC-RDDC@drdc-rddc.gc.ca.

- © Her Majesty the Queen in Right of Canada (Department of National Defence), 2018
- © Sa Majesté la Reine en droit du Canada (Ministère de la Défense nationale), 2018

CAN UNCLASSIFIED

Abstract

A procedure has been developed to enable target geolocation information to be processed from data collected over a wide surveillance area in which the effect of the Earth's surface curvature is notable. The surveillance area of interest on the curved surface and its associated air space are transformed from the ellipsoidal (world geodetic) frame with coordinates given in latitude, longitude and altitude to an appropriate Cartesian frame with coordinates given by x , y , z . The Cartesian coordinate system permits a simpler three-dimensional model for processing of the target's locations. It also allows a geometric approach to be used to solve the TDOA equations, using hyperboloids as solutions to the TDOA problem. The appeal of the geometric approach is its applicability in target geolocation processing using data collected from a minimum number of receivers deployed in a passive detection system as discussed in a previous study in [1].

Results have shown that the TDOA processing procedure developed in this study can provide proper target localization over a curved segment of the Earth's surface. TDOA processing over a wide surveillance area is desirable in a practical passive detection system. It enables a reduction in the overall detection system's physical complexity by reducing the minimum number of receivers deployed, thereby reducing the amount of data to be collected and processed.

Significance to defence and security

One of the future challenges in Intelligence, Surveillance and Reconnaissance (ISR) applications for the Canadian Armed Forces (CAF) is to monitor air activities over the vast area of the Canadian Arctic region. Some of these activities could pose threats to Canada's sovereignty and national economic interest. A passive sensing system that exploits the target's radio-frequency (RF) emission offers a promising and viable sensing technology that can be exploited as an ISR capability. It can provide the CAF with reliable, real-time warning of any breach in security and air defence.

Given the vast area of the Canadian Arctic, and the logistical challenges of providing reliable support to maintain surveillance operations, it is imperative that the complexity of the surveillance system be reduced to a minimum. A surveillance system that can cover as large an area as possible by leveraging the detection limit of the sensors, thereby reducing the total number of sensors deployed, will reduce the complexity of the surveillance system network and hence improve the system's operational robustness. Accordingly, it requires the development of an appropriate sensor configuration and processing procedure to adapt to such a physical layout of the network system, but still enabling relevant ISR information to be extracted accurately.

Résumé

On a élaboré une procédure permettant le traitement de données de géolocalisation de cibles à partir des données de surveillance recueillies au-dessus d'un vaste territoire où l'effet de l'incurvation de la surface terrestre est perceptible. La zone de surveillance d'intérêt sur la surface incurvée et son espace aérien connexe est transformée d'un cadre ellipsoïdal (géodésique mondial) avec coordonnées exprimées en latitude, longitude et altitude en un cadre cartésien avec coordonnées exprimées en x , y , z . Le système de coordonnées cartésiennes constitue un modèle tridimensionnel simplifié pour le traitement de l'emplacement des cibles. Il permet également l'utilisation d'une approche géométrique pour la résolution des équations TDOA. Il permet notamment l'utilisation d'hyperboloïdes comme solutions au problème de TDOA. L'avantage de l'approche géométrique réside dans la possibilité de l'utiliser pour la géolocalisation de cibles à partir de données recueillies par un nombre minimal de récepteurs déployés dans un réseau de détection passif, tel qu'abordé dans une étude antérieure [1].

Les résultats ont démontré que la procédure de traitement TDOA élaborée dans le cadre de cette étude permet de localiser efficacement une cible au-dessus d'un segment incurvé de la surface terrestre. Le traitement TDOA appliqué à une vaste zone de surveillance est souhaitable dans un système de détection passif. Il permet la réduction de la complexité physique du système de détection global en réduisant le nombre de récepteurs déployés, ce qui réduit la quantité de données à colliger et à traiter.

Importance pour la défense et la sécurité

L'un des prochains enjeux en matière de renseignement, surveillance et reconnaissance (RSR) pour les Forces armées canadiennes (FAC) sera de surveiller les activités aériennes dans la vaste région de l'Arctique canadien. Certaines de ces activités pourraient constituer une menace pour la souveraineté du Canada ou les intérêts économiques nationaux du pays. Un système de détection passive exploitant les émissions radiofréquences (RF) de cibles potentielles offre une solution technologique de détection prometteuse et viable pouvant être exploitée dans le cadre d'une capacité de RSR. Cette solution peut fournir aux FAC un avertissement fiable en temps réel de toute atteinte à la sécurité et de toute violation de l'espace aérien.

Compte tenu de l'immensité du territoire arctique canadien et des défis logistiques associés à sa surveillance en continu, il est crucial que la complexité du système de surveillance soit réduite au strict minimum. La mise en œuvre d'un réseau de surveillance capable de couvrir la plus grande zone possible en tirant profit des seuils de détection des capteurs, réduisant ainsi le nombre de capteurs totaux déployés, permettra de réduire la complexité du réseau de surveillance et améliorera ainsi la robustesse opérationnelle du système. Pour ce faire, les capteurs du réseau doivent être configurés en conséquence, et une procédure de traitement doit être élaborée afin d'adapter le système à un tel déploiement physique tout en autorisant l'extraction précise des informations de RSR.

Table of contents

Abstract	i
Significance to defence and security	i
Résumé	ii
Importance pour la défense et la sécurité	ii
Table of contents	iii
List of figures	iv
List of tables	v
1 Introduction	1
2 TDOA method	3
2.1 TDOA for passive target localization	3
2.2 TDOA equations for determining target location	4
2.3 Geometric approach	4
3 TDOA processing over a curved surface	8
3.1 Earth coordinate systems	8
3.2 Local geodetic coordinate systems	9
3.3 Global Cartesian frame for a non-coplanar receiver system	11
3.4 TDOA processing in global Cartesian coordinate frame	16
4 Target localization	18
4.1 Target surveillance scenario	18
4.2 Target localization process	20
4.3 Target localization results	22
5 Conclusions	25
References	26
List of symbols/abbreviations/acronyms/initialisms	28

List of figures

Figure 1:	Passive sensing system configuration in Cartesian coordinates; a) plan view, b) three-dimensional view.	3
Figure 2:	A pair of receivers (S1–S2) and a target are situated in a two-dimensional plane in the local coordinate frame.	5
Figure 3:	Hyperboloids in local coordinate frame (x',y',z') in three dimensions.	6
Figure 4:	A hyperboloid representing the TDOA of an air target as detected by a pair of receivers in local coordinate frame.	7
Figure 5:	Location of a point on an elliptical Earth in world geodetic coordinates (ϕ,θ,h) and conventional terrestrial coordinates (X,Y,Z)	8
Figure 6:	a) Great-circle arc length between two points on the surface of a spherical Earth; b) Arc length D and chord length d between two points on a great-circle.	9
Figure 7:	Conventional terrestrial coordinates (X,Y,Z) to local geodetic coordinates (N,E,U)	10
Figure 8:	Re-labelling the local geodetic frame $(N,E,U)=(x,y,z)$ to the conventionalized local geodetic frame $(E,N,U)=(x',y',z')$	11
Figure 9:	Tangent plane (red) defined at receiver-S1 in the conventionalized local geodetic frame.	11
Figure 10:	Conventionalized local geodetic frame (x',y',z') with tangent plane $(x'-y')$ at receiver S1.. . . .	13
Figure 11:	Rotating the $(x'-y')$ plane about the z' -axis (in Figure 10) to the $x''-y''$ plane above receiver S4.	13
Figure 12:	Rotating the $(x''-z'')$ plane about the y'' -axis (in Figure 11) to the $u''-w''$ plane with the u'' -axis touching receiver S4.	14
Figure 13:	Rotating the $(u''-v'')$ plane about the u'' -axis (in Figure 12) to the $x-y$ plane. S1, S3 and S4 are points on the $x-y$ plane (light orange); S2 is above the $x-y$ plane.	15
Figure 14:	Sequence of frame transformation through various stages, from world geodetic coordinates (lat,lon,alt) to the standard Cartesian coordinates (x,y,z)	16
Figure 15:	a) intersection of 3 hyperboloids; b) an enlarged view of the intersection region.	17
Figure 16:	A passive detection unit of 4 receivers and the area of surveillance (red box).	18
Figure 17:	Target localization results from TDOA measurements. Open black circles = ground truth; red diamonds = computed target locations.	22
Figure 18:	Target locations displayed on Google Earth map. Yellow = ground truths. Green = computed.	24

List of tables

Table 1:	Receiver operating parameters.	19
Table 2:	Locations of the four receivers in world geodetic coordinates and global Cartesian coordinates.	20
Table 3:	TDOA measurement values d_{ij} for receiver-pairs (S1–S2), (S3–S4) and (S1–S4) at 10 sampling times along the target’s flight path in Figure 16.	20
Table 4:	Results of target localization in the global Cartesian coordinate frame (x,y,z).	23
Table 5:	Results of target localization in the world geodetic coordinate frame (lat,lon,alt).	24

This page intentionally left blank.

1 Introduction

Passive target detection and localization methods are widely used in many applications, such as navigation, search and rescue, surveillance and electronic warfare. A well-established method used in passive target location is the time-difference-of-arrival (TDOA) technique that exploits the radio-frequency (RF) transmission of the target. For example, this passive detection method can be particularly useful for detecting small drones; the RF emissions from the first-person-view cameras used for remote-piloting the drones can be exploited.

The TDOA method for determining the location of a target is a line-of-sight (LOS) process. This approach is best described by a model in which the locations of the targets and the receivers are specified in a Cartesian coordinate system. That is, the TDOA analysis is performed by assuming a flat-Earth approximation. It is found that virtually all the developments of the TDOA modeling process are based on the Cartesian coordinate system. It is the simplest and most appropriate frame of reference to use because of the LOS characteristics of RF signal propagation.

The flat-Earth assumption may be a good approximation and adequate for analyzing the TDOA process over a small surveillance area where the Earth's surface can be considered as more or less flat. For surveillance covering a large area, the curvature of the Earth's surface will introduce noticeable deviation to the flat-Earth approximation. For example, an air target flying at a constant altitude over a long distance above the Earth's surface will trace out a curved path in a Cartesian frame. This is manifested as a continuing change in the height of the target in the Cartesian coordinate frame. The target would initially appear on the horizon when it is far away, then rise up in height as it approaches the detection system.

Another effect of a passive detection system covering a large surveillance area is that the separation distance between receivers in the passive system is no longer the distance (arc length) measured along the surface of the Earth as in the flat-Earth approximation; rather, it is the "line-of-sight" distance (chord length) between receivers situated on the Earth's curved surface. Thus, adjustments will have to be made to set up the TDOA analysis properly in the Cartesian coordinate frame in order to extract target location information correctly.

It can be argued that a vast surveillance area can be subdivided into smaller parcels of areas so that the TDOA process can be handled by a flat-Earth approximation. This may at first be seen as a logical approach to the problem of passive surveillance over a large area. However, it is neither viable nor practical; smaller area patches imply that a larger number of passive detection units must be deployed, one for each smaller area patch. Hence, a large number of receivers will be required and a larger volume of data will need to be collected and processed. This will increase both the hardware and software complexity of the detection system, presenting a number of challenges. A data transferring system must be able to provide sufficient capacity to upload a large amount of data from all the receiver sites to a central processing site and more computing resources must also be provided to process the large volume of data. Thus from the operational point of view, it is desirable to deploy a minimum number of receivers to keep the system complexity low and acquire less data to process, making the system more robust and capable of real-time operation. This means it would be preferable to have a passive detection unit that can cover as large a surveillance area as possible, up to the technical limit of the receiver's detection range.

Thus a TDOA processing procedure that can handle curved-surface geometry is required to facilitate the computation of the target location properly.

It is expected there will be increasing foreign surveillance activities in the Arctic creating various sovereignty-related threats and challenges to Canada. One of the likely scenarios expected in the Arctic in the near future is increasing exploration activities, especially in prospecting for natural resources by multi-national corporations [2]. Remote natural resources prospecting by drones or small aircraft will become common occurrence due to the advance in remote sensing technology [3]. As a situational awareness tool to detect these potential activities, passive detection system can be set up to monitor a large sensitive area that is deemed to be prone to unwanted hostile surveillance activities.

Drone equipped with a typical First Person View transmitter of about 1W for remote-piloting can be detected and geolocated, with a modest coherent signal integration gain of 10 in the SNR (signal-to-noise ratio), by the TDOA method out to 30 km. At this distance, the effect of the Earth's curvature will become noticeable in the TDOA process, affecting the target's height and the separation distances among the receivers in the passive detection unit. As an illustration, a drones flying at an altitude of 70m will be seen just on the horizon by a receiver at sea-level when the drone is about 30 km away, the maximum line-of-sight distance [4]. As the target approaches the receiver, it will appear to rise in height relative to the horizon, up to a height of 70m as it passes directly over the receiver.

In the case of a manned aircraft, it is required by international protocol to carry an IFF (Identification Friend or Foe) transponder broadcasting its location and identifying itself through ADB-S signals (Automatic Dependent Surveillance-Broadcast). A typical commercial IFF transponder transmits a power of around 100 W at the low end for aircraft flying below 5000 m in altitude [5]. A 100W ADB-S transponder signal corresponds to a detection stand-off distance of about 450 km as a conservative estimate. Thus a large swathe of airspace can be monitored by detecting the ADB-S signal for any sign of intrusion, and preferably deploying only a single passive detection unit to keep the number of receivers required for TDOA processing to a minimum and hence the detection system's complexity low. Most natural-resource prospecting flights by foreign entities will likely be done discretely to avoid any attention. Since turning-off the IFF transponder may have negative consequences and may not be a preferred option, spoofing the ADB-S signals by broadcasting erroneous locations of the aircraft is one way to conceal its true locations. Passive detection monitoring a large area can exploit the ADB-S signal transmission to circumvent IFF deception and provide a situational awareness of any suspicious surveillance activities over a sensitive area.

In this report, a procedure has been developed to process TDOA data to detect and track targets that appear in a large volume of airspace over an area using a single passive detection unit composed of four receivers. The effect of the curvature of the Earth that gives rise to variations in the target height and alters the geometry of the receivers relative to the targets will be taken into account. Target flight paths and receiver locations given by curved space coordinates in terms of latitude, longitude and altitude (world geodetic coordinates) are converted to an appropriate Cartesian frame, enabling target localization to be determined using the geometric-approach TDOA method described in [1]. The targets' locations are then converted back to the world geodetic coordinates which human operators can understand readily.

2 TDOA method

2.1 TDOA for passive target localization

Passive location of a transmitting target using the TDOA method has been described and analyzed extensively in the literature for more than four decades [6]. The TDOA method is based on the principle of locating a target along a three-dimensional geometrical surface where the time difference of arrival of a target signal between a pair of synchronized receivers is constant. This surface is described by a hyperboloid. Using a group of four receivers stationed at different locations, three independent TDOA measurements can be made [7]. The TDOA measurements are then converted to hyperboloid surfaces. The intersecting point formed by the three hyperboloids determines the target's location in three-dimensional space.

In order to provide a clear illustration of how TDOA measurements can be made, a typical ground receiver configuration is used for illustration; this is shown in Figure 1. There are four receivers (S1, S2, S3, S4) in a passive detection unit. The receiver system in Figure 1 is configured in a “forward looking” mode, i.e., the receivers are monitoring the airspace at the top of Figure 1a (yellow shaded area). Also, the receivers are assumed to have a wide field of view in azimuth and elevation so that all four receivers monitor the same volume of airspace at the same time in staring-mode. The receiver locations are described in three dimensions by the Cartesian coordinates, (x,y,z) , giving the passive system a three-dimensional geometry.

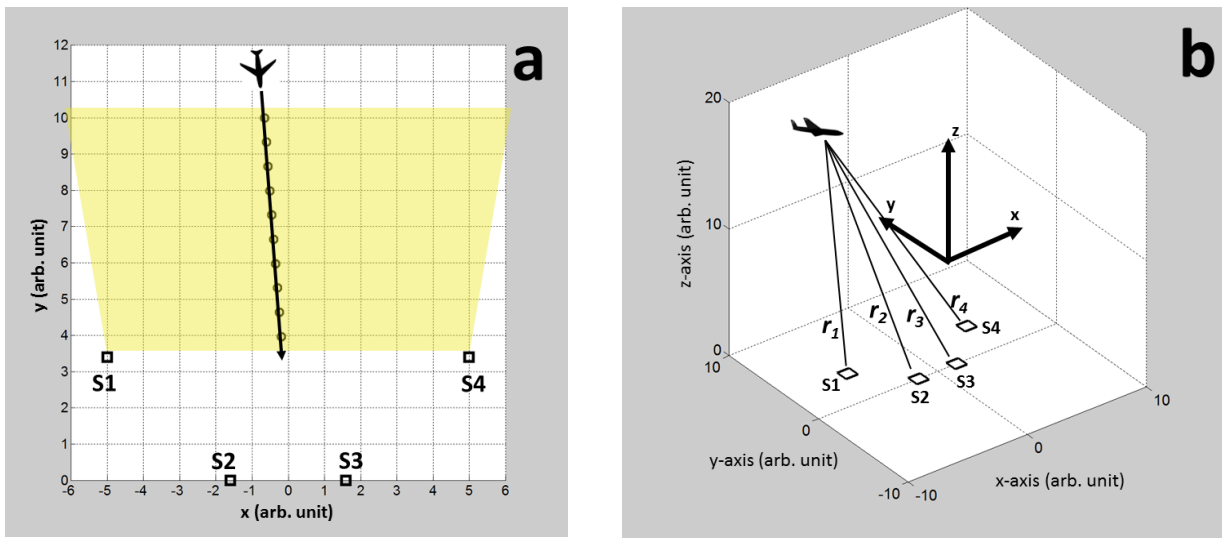


Figure 1: Passive sensing system configuration in Cartesian coordinates; a) plan view, b) three-dimensional view.

2.2 TDOA equations for determining target location

Three time-synchronized coherent receiver-pairs, S1–S2, S3–S4, and S1–S4 are formed from a group of four receivers in Figure 1 to collect three independent sets of TDOA measurement data. Three independent TDOA measurements are needed to locate a target. For example, TDOA τ_{12} is measured by the receiver-pair S1–S2, TDOA τ_{34} by the receiver-pair S3–S4 and TDOA τ_{14} is measured by the receiver-pair S1–S4. The set of three TDOA equations are,

$$\begin{aligned} d_{12} &= c\tau_{12} = r_1 - r_2 \\ d_{34} &= c\tau_{34} = r_3 - r_4 \\ d_{14} &= c\tau_{14} = r_1 - r_4 \end{aligned} \quad (1)$$

where $d_{ij} = c\tau_{ij}$ is the range-difference from the target to receiver i and receiver j . c is the speed of light; $r_i = ((x - x_i)^2 + (y - y_i)^2 + (z - z_i)^2)^{1/2}$ is the L_2 -norm (Euclidean) distance between the target (x,y,z) and receiver (x_i, y_i, z_i) (see Figure 1b) and $i, j = 1, 2, 3, 4$. For simplicity and consistency, d_{ij} will be referred to as the ‘‘TDOA measurement.’’ Each of the equations in Equation (1) represents a three-dimensional hyperboloid surface geometrically; this will be discussed in more detail in Section 2.3. Since the receiver positions (x_i, y_i, z_i) are known and the TDOA measurement values d_{ij} are available, Equation (1) with three independent equations can be solved for the three unknown target location coordinates (x,y,z) to find the target location with the proper receiver geometry [1].

The TDOA equations in Equation (1) are solved using a geometric approach. This approach offers a simpler algorithm for multi-target localization as discussed in [1].

2.3 Geometric approach

Geometrically, Equation (1) describes three intersecting hyperbolic surfaces. A geometry-based method generates three hyperboloids from the three equations in Equation (1) and then looks for the intersection region from the three hyperboloids as the solution for target location. Mathematically, the geometric form of each hyperboloid in Equation (1) can be described more simply by considering each pair of receivers in its own local coordinate frame of reference. This is to distinguish it from the common coordinate frame in which all the receivers and targets must reside in order to determine the target location; this common frame shall be called the global coordinate frame.

Receiver-pair S1–S2 will be used as an illustrative example. In the local frame, the receiver-pair separated by a distance d is placed on the x' -axis symmetrically. That is to say, receiver S1 has the coordinate $(x', y', z')_1 = (-d/2, 0, 0)$, and receiver S2 has the coordinate $(x', y', z')_2 = (d/2, 0, 0)$. Furthermore, the y' -axis is oriented such that the target is situated in the x' - y' plane; i.e., with coordinates $(x', y', 0)$. Thus, a local frame is defined in which the two receivers and the target are all confined in a two-dimensional plane (i.e., x' - y' plane). This is illustrated schematically in Figure 2.

Using the first equation in Equation (1) for the S1–S2 receiver-pair, and substituting in the receivers and target coordinates,

$$\begin{aligned}
d_{12} &= r_1 - r_2 \\
&= \sqrt{(x' - x_1')^2 + (y' - y_1')^2} - \sqrt{(x' - x_2')^2 + (y' - y_2')^2} \\
&= \sqrt{\left(x' + \frac{d}{2}\right)^2 + y'^2} - \sqrt{\left(x' - \frac{d}{2}\right)^2 + y'^2}
\end{aligned} \tag{2}$$

After some algebraic rearrangements, Equation (2) can be re-expressed as,

$$\frac{x'^2}{\left(\frac{d_{12}^2}{4}\right)} - \frac{y'^2}{\left(\frac{d^2}{4} - \frac{d_{12}^2}{4}\right)} = 1 \tag{3}$$

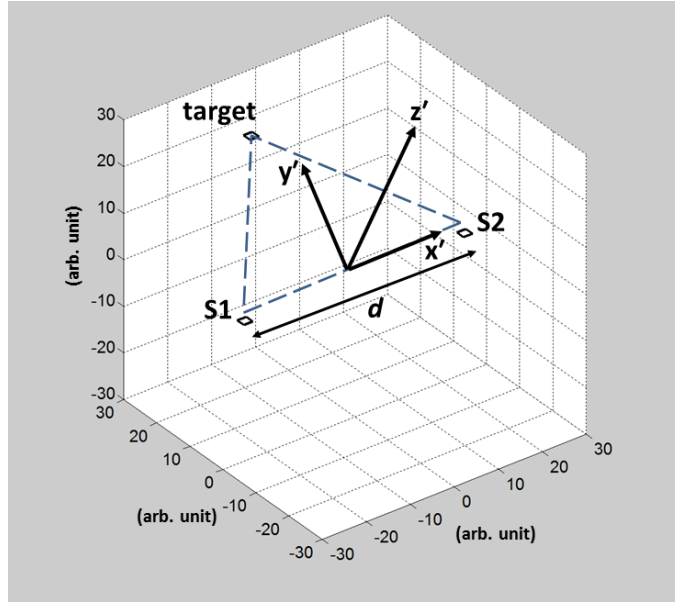


Figure 2: A pair of receivers (S1–S2) and a target are situated in a two-dimensional plane in the local coordinate frame.

Equation (3) is a “hyperbola of two-sheet” in two dimensions [8]. A three-dimensional hyperboloid can be generated by the method of volume of revolution about the x' -axis. The hyperboloid is thus given by,

$$\frac{x'^2}{a^2} - \left(\frac{y'^2}{b^2} + \frac{z'^2}{b^2}\right) = 1 \tag{4}$$

where $a = (d_{12}/2)$, $b = (d^2 - d_{12}^2)^{1/2}/2$, $d > d_{12}$. Physically, the hyperboloid surface represents an isochrone where a point anywhere on the surface has the same TDOA with respect to receivers S1 and S2. Recasting Equation (4) in the form,

$$x' = \pm |a| \left(1 + \left(\frac{y'^2}{b^2} + \frac{z'^2}{b^2} \right) \right)^{1/2} \quad (5)$$

it can be seen that there are two distinct hyperboloid surfaces that can exist; one has $+|a|$ value and the other has $-|a|$ value in Equation (5). These two hyperboloids are shown in Figure 3. Moreover, because the hyperboloid is a surface generated from volume of revolution about the x' -axis, it is therefore symmetrical in a rotation about the x' -axis. Thus, the local frame axes are defined with the z' -axis as pointing vertically upward as illustrated in Figure 3.

Recall from Equation (4) that the parameter a , is just the TDOA measurement value d_{12} multiplied by a factor of $1/2$. The TDOA measurement value can take on either positive or negative value; this can be clearly seen from Equation (2). If the target is closer to receiver S2 than to receiver S1, then a is positive because $d_{12} = r_1 - r_2$ is positive; otherwise, a is negative. When the target is exactly the same distance from both receivers (i.e., $a = 0$), Equation (5) degenerates into a plane described by $x' = 0$.

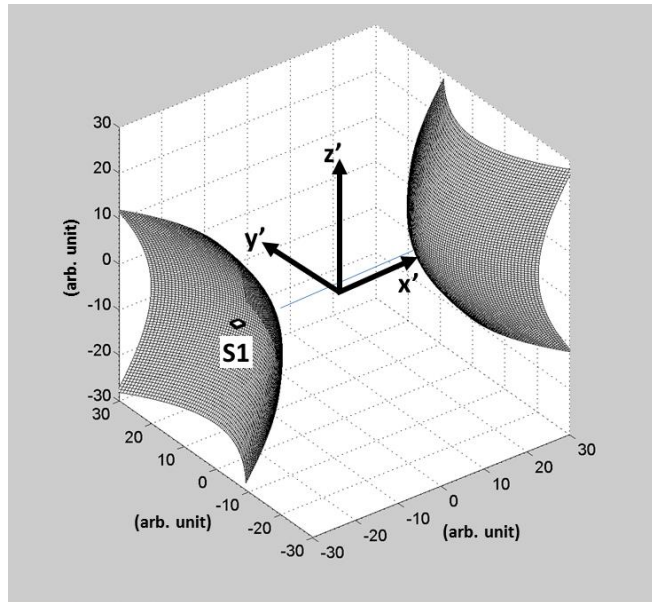


Figure 3: Hyperboloids in local coordinate frame (x',y',z') in three dimensions.

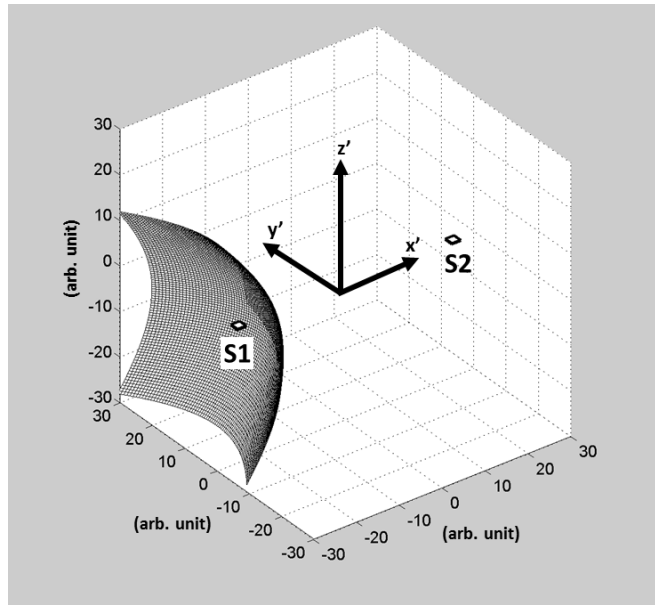


Figure 4: A hyperboloid representing the TDOA of an air target as detected by a pair of receivers in local coordinate frame.

The TDOA measurement d_{12} of a target will have either a plus or minus sign associated with it. Therefore, only one of the two hyperboloids in Figure 3 is valid. If the TDOA measurement value d_{12} is negative (i.e., $r_1 < r_2$), only the hyperboloid closer to receiver S1 is valid; this is shown in Figure 4. Thus the geometric solution automatically constrains the solution to the correct sector of the airspace volume. In effect, the hyperboloid surface shown in Figure 4 represents the solution to each of the TDOA equations in Equation (1).

Hyperboloids for receiver-pairs S3–S4 and S1–S4 can be obtained in the exact same manner in their own local coordinate frame (x', y', z') . The three hyperboloids will then be relocated to the common global coordinate frame (x, y, z) and properly oriented relative to their respective receiver-pairs so that the intersection of the three hyperboloid, and hence the target location can be determined. The re-orientation of the local frame to the global frame of the three hyperboloids is discussed in detail in [1].

3 TDOA processing over a curved surface

3.1 Earth coordinate systems

The locations of the target and receivers are conventionally given in world geodetic coordinates (i.e., latitude, longitude, altitude) to reflect the curvilinear geometry of the earth. As discussed in Section 2, the TDOA problem that provides target localization in three-dimensional positioning is generally carried out in a Cartesian coordinate frame. The Cartesian frame is simpler, more intuitive, and easier to work with mathematically; the use of curvilinear coordinates results in more complicated models [9]. Thus to model and analyze the TDOA process of a target moving over the Earth across a large surface area, the world geodetic coordinates are converted to an appropriate Cartesian frame through a series of coordinate frame transformation. This is the objective of the discussion in this section. First, the world geodetic coordinates are converted to the Earth-centred, Earth-fixed conventional terrestrial Cartesian coordinates, (X, Y, Z) . Modelling the Earth as an ellipsoid [p.100, 9] [10], the conventional terrestrial coordinates are given by

$$\begin{aligned} X &= (N + h) \cos \phi \cos \lambda \\ Y &= (N + h) \cos \phi \sin \lambda \\ Z &= ((1 - e^2)N + h) \sin \phi \end{aligned} \tag{6}$$

where ϕ is the ellipsoidal geodetic latitude, λ is the ellipsoidal geodetic longitude, h is the height above the ellipsoid surface (altitude), $N = a/(1 - e^2 \sin^2 \phi)^{1/2}$, a is the ellipsoid's major semi-axis, and e is the ellipsoid's eccentricity. For the coordinate system WGS84 (World Geodetic System), $a = 6378.137$ km and $e = 0.0818$. WGS84 is a standard adopted for GPS applications.

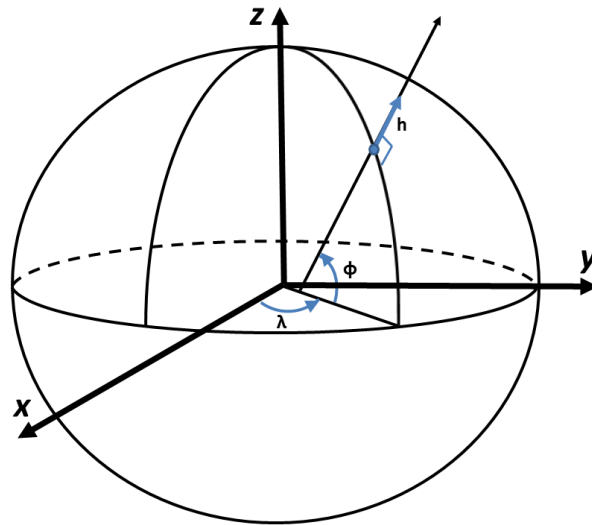


Figure 5: Location of a point on an elliptical Earth in world geodetic coordinates (ϕ, θ, h) and conventional terrestrial coordinates (X, Y, Z) .

Figure 5 illustrates the relationship between the world geodetic coordinates (ϕ, λ, h) and the conventional terrestrial coordinates (X, Y, Z) . Note that for the geodetic latitude in the ellipsoidal coordinates, the normal at a point on the surface of an ellipsoid does not pass through the centre of the ellipsoid except for points on the equator or at the two poles [11].

Over a small segment of the curved surface on Earth, the arc length D between 2 points on the surface of the Earth (P_1 and P_2), where the subtended angle α is small compared to 2π as shown in Figure 6a, can be approximated by a great-circle arc length by assuming a spherical Earth. This is illustrated in Figure 6b. It is obvious from Figure 6b that the chord length d between P_1 and P_2 is different from the arc length when the curvature effect of the Earth is notable. In the TDOA process to localize the target, the line-of-sight chord length d is the appropriate length to be used as the separation distance between two receivers, and it is simply given by,

$$d = ((X_2 - X_1)^2 + (Y_2 - Y_1)^2 + (Z_2 - Z_1)^2)^{1/2} \quad (7)$$

where (X_1, Y_1, Z_1) and (X_2, Y_2, Z_2) are the locations of points P_1 and P_2 respectively in the conventional terrestrial coordinate frame.

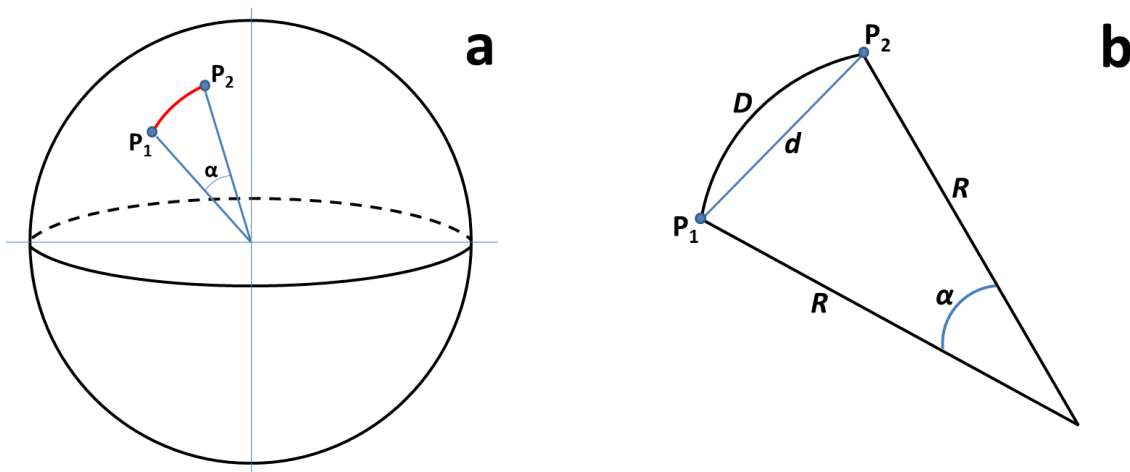


Figure 6: a) Great-circle arc length between two points on the surface of a spherical Earth; b) Arc length D and chord length d between two points on a great-circle.

3.2 Local geodetic coordinate systems

In targeting and tracking applications, a local geodetic coordinate system is adopted from the conventional terrestrial coordinate (X, Y, Z) system [9]. This local geodetic system is a Cartesian coordinate system that has a chosen reference point as the origin located on the Earth's surface. The coordinate axes are x pointing to the North (N), y pointing to the East (E) and z pointing up (U); i.e., $(x, y, z) = (N, E, U)$ [9, 12]. This is shown in Figure 7. The x - y plane is tangent to the Earth's surface ($h = 0$ in Equation (9)) at the reference point; the z -axis (U) is normal to the ellipsoidal Earth at the reference point with $z = 0$. In other words, the reference point serves as the origin $(x, y, z) = (0, 0, 0)$ of the local geodetic system.

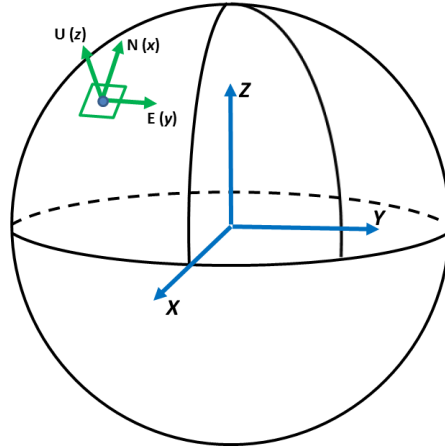


Figure 7: Conventional terrestrial coordinates (X, Y, Z) to local geodetic coordinates (N, E, U) .

The transformation of any point from the conventional terrestrial frame (X, Y, Z) to the local geodetic frame (x, y, z) is given by [9,10,12],

$$\begin{pmatrix} x \\ y \\ z \end{pmatrix} = \begin{pmatrix} -\sin \phi \cos \lambda & -\sin \phi \sin \lambda & \cos \phi \\ -\sin \lambda & \cos \lambda & 0 \\ \cos \phi \cos \lambda & \cos \phi \sin \lambda & \sin \phi \end{pmatrix} \begin{pmatrix} X - X_0 \\ Y - Y_0 \\ Z - Z_0 \end{pmatrix} \quad (8)$$

where (X_0, Y_0, Z_0) is the conventional terrestrial frame coordinates of the reference point $(x, y, z) = (0, 0, 0)$ in the local geodetic frame. For example, receiver-S1 of the passive detection system (Figure 1) is chosen as the reference point. The other three receivers of the passive detection system and any targets can then be assigned a location with coordinates (x, y, z) in the local geodetic frame.

However, there is still a misalignment between the local geodetic coordinates and the standard Cartesian coordinates used in the TDOA equation in Equation (1). The local geodetic coordinates have the x -axis pointing North and the y -axis pointing East; i.e., $(x, y, z) = (N, E, U)$. Whereas, the standard Cartesian coordinate frame has the x -axis pointing East and the y -axis pointing North. The standard Cartesian coordinate frame is required to conduct TDOA processing. This can be remedied simply by interchanging the x -axis and y -axis of the local geodetic frame in the standard Cartesian frame convention; this simple procedure can be justified in vigor mathematically [13],

$$\begin{aligned} x' &= y \text{ (East)} \\ y' &= x \text{ (North)} \\ z' &= z \text{ (Up)} \end{aligned} \quad (9)$$

This is depicted in Figure 8. Equation (9) has the same Cartesian axes orientation as the TDOA equations in Equation (1); i.e., $(x', y', z') = (E, N, U)$.

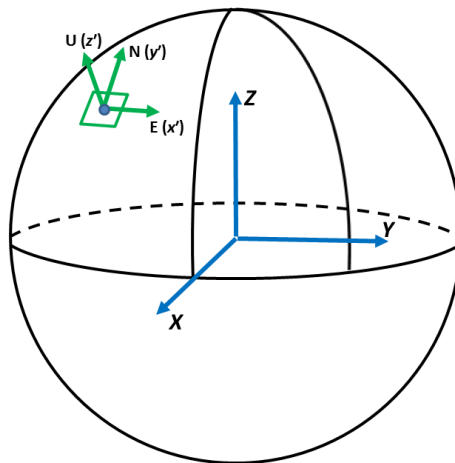


Figure 8: Re-labelling the local geodetic frame $(N,E,U)=(x,y,z)$ to the conventionalized local geodetic frame $(E,N,U)=(x',y',z')$.

3.3 Global Cartesian frame for a non-coplanar receiver system

For a passive detection cell composed of 4 receivers located on the Earth's surface, it would appear that each receiver is located at a different height z' . This is because receiver-S1 as the reference point defines the tangent plane $x'-y'$ of the conventionalized local geodetic (E,N,U) frame in Equation (9). The origin $(x',y',z') = (0,0,0)$ is in fact the highest point on the Earth's surface in the (E,N,U) frame; any other points on the Earth's surface will be beneath the tangent plane defined at $(x',y',z') = (0,0,0)$. Figure 9 illustrates the tangent plane (red) at receiver-S1 and other receiver locations relative to receiver-S1 in the (x',y',z') frame. The tangent plane $(x'-y')$ extends perpendicularly out of the page in Figure 9.

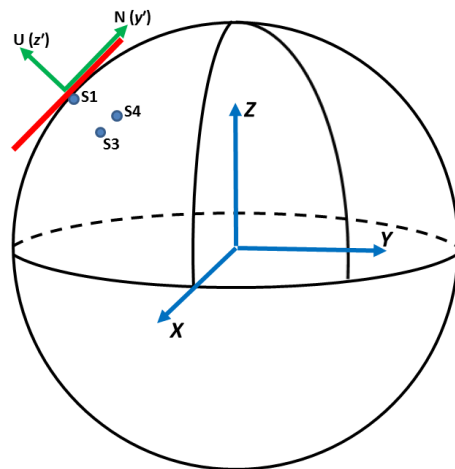


Figure 9: Tangent plane (red) defined at receiver-S1 in the conventionalized local geodetic frame.

It has been discussed in [1] that the TDOA process requires a non-coplanar four-receiver configuration; that is, one of the four receivers should not be on the same plane as the other three receivers. It should be noted that any three non-collinear points (i.e., three receivers) located arbitrarily in three dimensional space will form a plane. Hence, the fourth receiver must be located either above or below this plane. In the case of the “flat-Earth” approximation, three receivers would be located on the x' - y' tangent plane which describes the Earth’s surface; the fourth receiver would be situated above the “flat-Earth’s” surface (i.e., altitude > 0).

A proper working coordinate frame to conduct the TDOA analysis on a curved surface is defined by re-orienting the tangent plane in Figure 9 such that the tangent plane contains three of the four receivers. That is, the locations of receiver-S1, S3, S4 in Figure 1 are chosen to be located on this plane. This plane is obtained by re-orienting the tangent plane at receiver-S1 as illustrated in Figure 10 through a series of three rotations. First, the x' - y' tangent plane as shown in Figure 10 is rotated about the z' -axis by an amount θ towards receiver-S4 such that the rotated x' -axis is located right on top of receiver-S4 to form a new coordinate frame,

$$\begin{aligned}x'' &= x' \cos \theta - y' \sin \theta \\y'' &= x' \sin \theta + y' \cos \theta \\z'' &= z'\end{aligned}\tag{10}$$

This is illustrated in Figure 11; the rotated angle θ is given by,

$$\begin{aligned}\theta &= -\tan^{-1} \left| \frac{y'_{rec4}}{x'_{rec4}} \right| \quad \text{if } y' \geq 0 \\ &= \tan^{-1} \left| \frac{y'_{rec4}}{x'_{rec4}} \right| \quad \text{if } y' < 0\end{aligned}\tag{11}$$

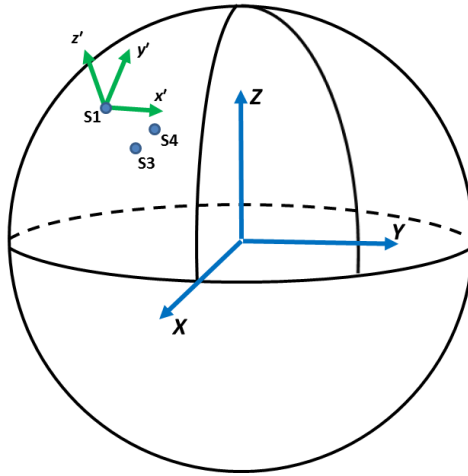


Figure 10: Conventionalized local geodetic frame (x',y',z') with tangent plane $(x'-y')$ at receiver $S1$.

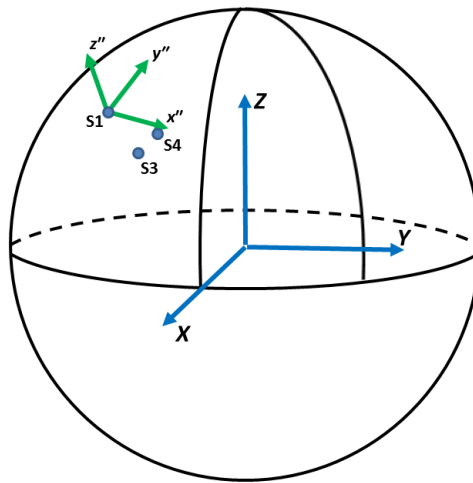


Figure 11: Rotating the $(x'-y')$ plane about the z' -axis (in Figure 10) to the $x''-y''$ plane above receiver $S4$.

Then, the $x''-z''$ plane in Figure 11 is rotated about the y'' -axis by an amount β such that the x'' -axis is touching receiver- $S4$ to form another new coordinate frame,

$$\begin{aligned}
 u'' &= x'' \cos \beta - y'' \sin \beta \\
 v'' &= y'' \\
 w'' &= x'' \sin \beta + y'' \cos \beta
 \end{aligned}
 \tag{12}$$

This is illustrated in Figure 12; the rotated angle β is given by,

$$\begin{aligned}
\beta &= -\tan^{-1} \left| \frac{z''_{rec4}}{x''_{rec4}} \right| && \text{if } z'' \geq 0 \\
&= \tan^{-1} \left| \frac{z''_{rec4}}{x''_{rec4}} \right| && \text{if } z'' < 0
\end{aligned} \tag{13}$$

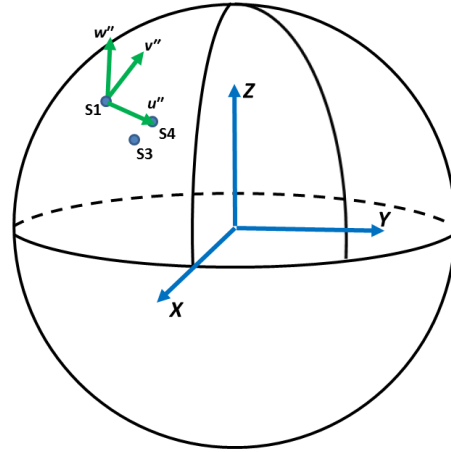


Figure 12: Rotating the $(x''-z'')$ plane about the y'' -axis (in Figure 11) to the $u''-w''$ plane with the u'' -axis touching receiver $S4$.

Receiver- $S4$ is now on the u'' -axis. Note that the new w'' -axis is no longer pointing straight up normal to the surface of the Earth at receiver- $S1$ due to the β -rotated tilt. Finally, the $u''-v''$ plane in Figure 12 is rotated by an amount γ about the v'' -axis to form the common global (x,y,z) coordinate frame such that receivers- $S1,S3,S4$ now all reside on the new x - y plane,

$$\begin{aligned}
x &= u'' \\
y &= v'' \cos \gamma - w'' \sin \gamma \\
z &= v'' \sin \gamma + w'' \cos \gamma
\end{aligned} \tag{14}$$

This is illustrated in Figure 13; the rotated angle γ is given by,

$$\begin{aligned}
\gamma &= -\tan^{-1} \left| \frac{w''_{rec3}}{v''_{rec3}} \right| && \text{if } w'' \leq 0 \\
&= \tan^{-1} \left| \frac{w''_{rec3}}{v''_{rec3}} \right| && \text{if } w'' > 0
\end{aligned} \tag{15}$$

Receiver-S1 has coordinates $S_1 = (x_1, y_1, z_1) = (0, 0, 0)$; receiver-S3 has the coordinates $S_3 = (x_3, y_3, z_3) = (x_3, y_3, 0)$ and receiver-S4 has the coordinates $S_4 = (x_4, y_4, z_4) = (x_4, 0, 0)$. That is, receivers-S1, S3, and S4 are three non-collinear points; but they are coplanar, situated on the plane given by $z = 0$.

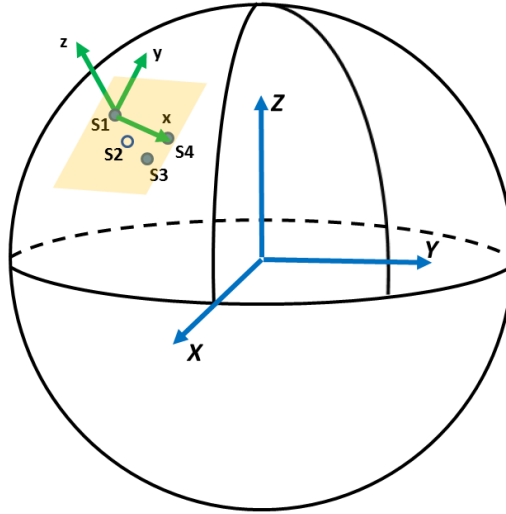


Figure 13: Rotating the (u'' - v'') plane about the u'' -axis (in Figure 12) to the x - y plane. S_1 , S_3 and S_4 are points on the x - y plane (light orange); S_2 is above the x - y plane.

Mathematically, three non-collinear points define a unique plane. Any point S on this plane can be described by the three known points as [14],

$$S = m_1 S_1 + m_3 S_3 + m_4 S_4 \quad (16)$$

where S is any point on the plane $z = 0$, and the coefficients m_1 , m_3 , m_4 take on all real values constrained by $m_1 + m_3 + m_4 = 1$.

For computing accurate three-dimensional target localization, a 4-receiver non-coplanar system configuration is required [1]. Since any three receivers located non-collinearly in three-dimensional space can form a plane, the fourth receiver S_2 in the detection system should be placed either above or below this plane where the three receivers are located.

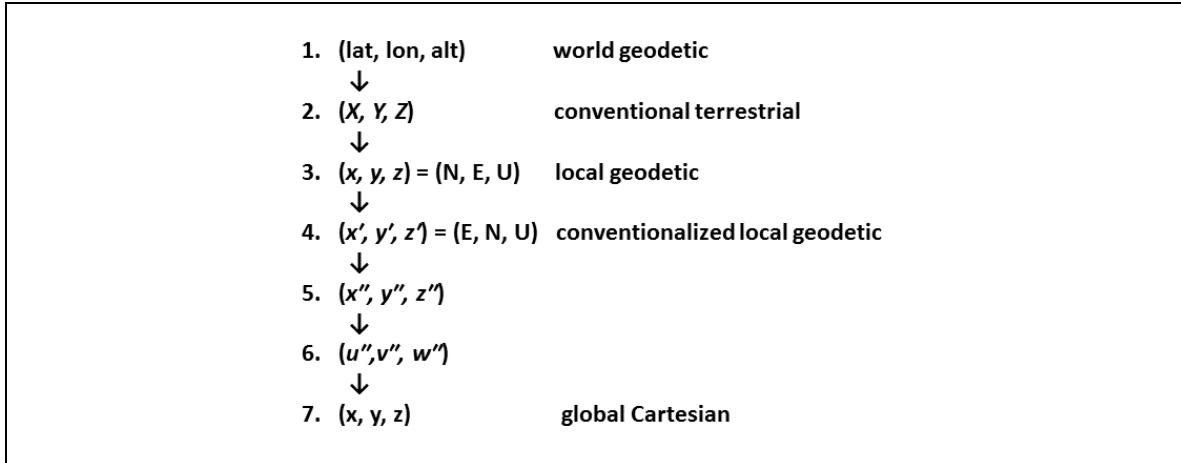


Figure 14: Sequence of frame transformation through various stages, from world geodetic coordinates (lat,lon,alt) to the standard Cartesian coordinates (x,y,z).

3.4 TDOA processing in global Cartesian coordinate frame

The sequence of coordinate transformation from (latitude, longitude, altitude) to (x,y,z) is illustrated in Figure 14. It should be noted that the global Cartesian frame gives the simplest geometry in processing the TDOA equation given in Equation (1). The two hyperboloids given by the coplanar receiver-pairs (S1–S4) and (S3–S4) can be transformed from their respective local frames (x',y',z') to the global Cartesian frame (x,y,z) by simple translation and rotation on the x-y plane as described in Section 2. The third hyperboloid that is obtained from the non-coplanar receiver-pair (S1–S2) requires an extra tilt rotation in the x-z plane in order to orient it properly geometrically with the two coplanar hyperboloids obtained from the receiver-pairs (S1–S4) and (S3–S4). This tilted hyperboloid has its associated z'-axis tilted as well in the rotation; hence the z'-axis grid marker will not be aligned with the z-axis grid marker in the global Cartesian frame. Thus, the tilted hyperboloid has to be re-graduated along the z-axis so that its z grid matches with those of the other two hyperboloids. The re-set of the z-axis grid graduation for receiver-pair (S1–S2) requires substantial computational time; this has been discussed in [1]. Figure 15 shows three properly oriented hyperboloids with respect to the receiver configuration set-up in the global Cartesian frame.

In contrast, the computational load is much greater if the local geodetic coordinate frame (E,N,U) in Figure 14 (the fourth stage in Figure 14) is used to process the three intersecting hyperboloids from receiver-pairs (S1–S2), (S3–S4), (S1–S4). This is because each of the three receiver-pairs is on a different plane in the (E,N,U) frame. The three sets of z'-axis grid graduation will have to be re-set so that the three hyperboloids would have a common z'-axis to facilitate the computing of the intersection properly.

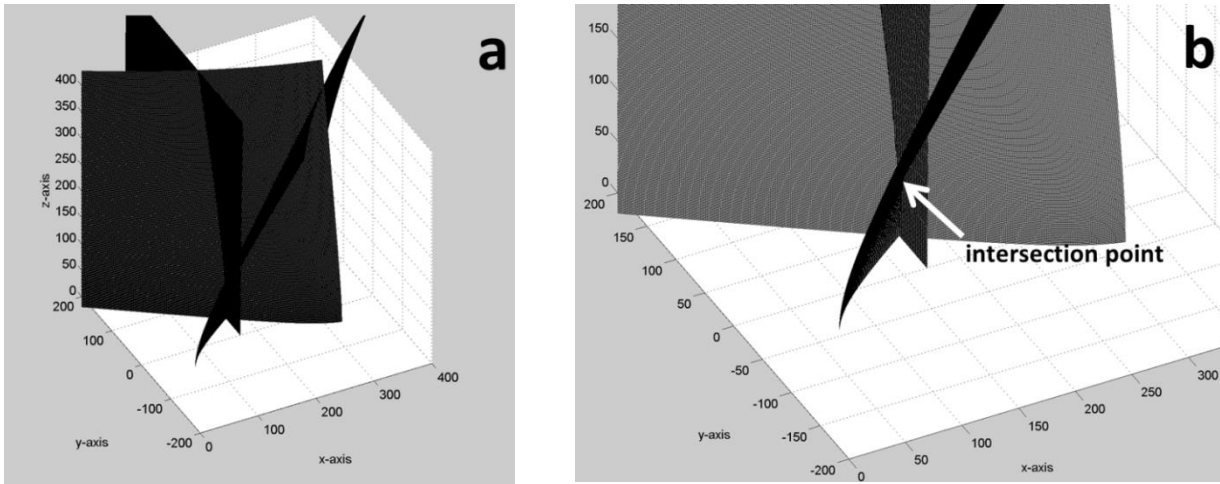


Figure 15: a) intersection of 3 hyperboloids; b) an enlarged view of the intersection region.

In brief, processing the TDOA measurements to find the target will produce the same geolocation results regardless which coordinate frame is being used. This is because the TDOA measurement between a target and the receivers are determined by the LOS distances, which are identical no matter which coordinate frame is being used. The (x,y,z) frame at the bottom of Figure 14 offers the best computational efficiency in target localization. It emulates the flat-Earth TDOA framework used in [1]. Thus, the (x,y,z) frame also offers a computing algorithmic procedure that has already been tried and established using the geometric approach described in Section 2. The geometric approach may be regarded as more practical as it requires data collected from only four receivers in the detection system in order to determine the three-dimensional location of a target. Whereas, other processing methods such as the algebraic approach discussed in [1] requires a five-receiver detection system. A detection system with fewer receivers is always preferable since it reduces the system hardware complexity and reduces the amount of data that need to be collected, uplinked and processed.

4 Target localization

4.1 Target surveillance scenario

A simulated scenario is used to illustrate TDOA processing for target localization from a large surveillance area where the effect of the earth's curvature will be taken into account. Under this scenario, the target's flight path will be a curved path following the curvature of the Earth's surface (i.e., an arc length) and the separation distance between receivers will be a LOS distance (i.e., a chord length) instead of the arc-length distance over the Earth's surface.

An area in the Northern part of Canada is used as an illustrative example to evaluate the TDOA process; this is shown in Figure 16. This area measures 340 km in length and 200 km in width. The area of surveillance is monitored by a single passive detection unit composed of 4 receivers. The narrower width of the surveillance area is constrained by the detection range of receiver S3, which must be able to cover the furthest corner of the red rectangular area. This is indicated by the white dot in Figure 16 which is located at the limit of the detection range of receiver-S3.

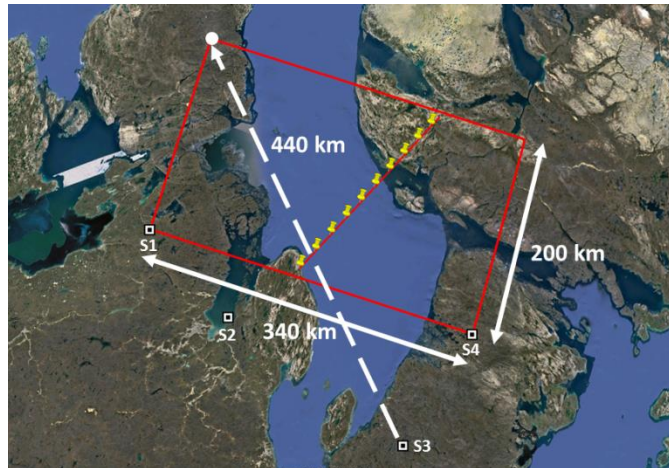


Figure 16: A passive detection unit of 4 receivers and the area of surveillance (red box).

The size of the surveillance area in Figure 16 corresponds to the case in which all the receivers in the passive detection unit can detect a small aircraft transmitting ADS-B signals of 100W from a commercial aviation IFF transponder [5], anywhere within the enclosed red box. Receiver detection range can be determined using the Friis transmission equation [15],

$$P_r = \frac{EIRP G_r \lambda^2}{(4\pi)^2 r^2 L} \quad (17)$$

where P_r is the RF signal power (W) detected by a receiver, $EIRP$ is the effective isotropic radiated power (W) of the transponder, G_r is the receiver antenna gain, λ is the wavelength (m) of the emitted RF signal,

r is the receiver's detection range (m), and L is the receiver's system loss factor. The noise power of a receiver is given by,

$$P_n = kT\beta \quad (18)$$

where P_n is the receiver noise power (W), k is the Boltzmann constant ($k = 1.38 \times 10^{-23}$ W/K/Hz), T is the receiver front-end noise temperature (K), and β is the noise bandwidth (Hz) which is taken to be the same as the signal bandwidth. A nominal noise temperature value $T = 344$ K is used for the receiver front-end. The signal bandwidth for an ADS-B signal is about 1 MHz [16]. This gives a system noise power of $P_n = 4.75 \times 10^{-15}$ W.

The signal-to-noise ratio (SNR) of a detected signal made by a receiver is given by,

$$SNR = \frac{P_r}{P_n} = \frac{EIRP G_r \lambda^2}{(4\pi)^2 r^2 L (kT\beta)} \quad (19)$$

For definitive detection of a signal, the SNR is nominally set at 40 such as in satellite phone applications (link margin 16dB) [17,18]. Using $SNR = 40$, Equation 19 gives a receiver detection range of $r = 440$ km for a ADS-B signal of 100 W. Table 1 summarizes the parametric values used in determining the receiver's detection range.

Table 1: Receiver operating parameters.

Signal <i>EIRP</i>	100 W
Signal bandwidth, β	1 MHz
Signal wavelength, λ (at $f = 1090$ MHz)	0.275 m
Receiver's field of view, <i>FOV</i>	100 degrees
Receiver antenna gain, G_r	3.3
Receiver noise power, P_n	4.75×10^{-15} W
Receiver system loss, L	4
Signal-to-noise ratio, <i>SNR</i>	40
Maximum receiver detection range, r	440 km

Thus it can be seen from Table 1 that any RF signal transmitted inside the red surveillance box can be adequately detected by all the receivers in the passive detection cell in Figure 16. Note that the distance between the white dot and receiver S3 in Figure 16 is 440 km, at the receiver's range detection limit. At this distance, the target had to be at a certain minimum altitude so that there is a line-of-sight established between the target and the most distant receiver. In the scenario, the target is assumed to be cruising at an altitude of 16 km. This altitude may seem a bit too high for a small plane, but this allows a large surveillance area scenario (200 km by 340 km) to be tested to validate the concept of TDOA processing over a curved surface on the Earth using a minimum number of four receivers.

In the scenario depicted in Figure 16, a small aircraft target is travelling south (downward), entering the red surveillance area from the north. The flight path is shown by a set of way-points. The way-points will be used as locations where the target's emitted signals will be sampled by the four receivers.

It has been mentioned in Section 3 that a non-coplanar receiver system configuration is needed to accurately provide three-dimensional target localization. To acquire a non-coplanar receiver configuration, receiver-S2 is placed at the location as shown in Figure 16. The Earth is assumed to have a flat terrain at sea-level; hence all four receivers are situated at sea-level. Taking advantage of the curvature of the Earth, the location of receiver-S2 ends up being 1812 m above the plane where receivers-S1, S3 and S4 are located in the (x,y,z) frame (bottom-most stage in Figure 14). The locations of the four receivers are shown in Table 2 in both the world geodetic coordinates (lat, lon, alt) and common global Cartesian coordinates (x,y,z).

Table 2: Locations of the four receivers in world geodetic coordinates and global Cartesian coordinates.

Receiver	(lat (deg), lon (deg), alt (m))	(x (m), y (m), z (m))
S1	(68.916, -92.641, 0)	(0, 0, 0)
S2	(68.500, -90.000, 0)	(100917, -58099, 1812)
S3	(68.000, -85.000, 0)	(304247, -125311, 0)
S4	(69.126, -84.266, 0)	(335345, 0, 0)

4.2 Target localization process

To validate the TDOA process for target localization in curved space, a target with a pre-defined flight path is used in the analysis. With known positions along the target's track, the TDOA measurements d_{ij} in the TDOA Equation (Equation (1)) can be calculated precisely with no error for the three receiver-pairs (S1–S2), (S3–S4) and (S1–S4) to create an ideal TDOA processing condition. By using the coordinate transformation procedure described in Section 3, and these error-free TDOA measurement values, target localization can be analyzed and used to definitively access TDOA processing over the Earth's curved surface. The TDOA measurement values d_{12} , d_{34} and d_{14} are calculated at 10 different way-point along the target's path, corresponding to samplings at 10 time instants during target's intrusion into the red surveillance area. These TDOA measurement values are tabulated in Table 3. Note that these TDOA measurements are irrespective of the coordinate frame used. They can be applied and processed in any of the coordinate frames shown in Figure 14; they are dependent only on the LOS distances between the target and the receivers as stated in Equation (1).

Table 3: TDOA measurement values d_{ij} for receiver-pairs (S1–S2), (S3–S4) and (S1–S4) at 10 sampling times along the target's flight path in Figure 16.

d_{12} (m)	d_{34} (m)	d_{14} (m)
22181.61	105337.02	84790.75
24485.53	100751.17	78118.68
27156.79	95172.41	70209.73
30283.09	88419.73	60853.48
33979.07	80323.40	49852.81
38395.38	70758.48	37063.06
43730.02	59687.21	22444.07
50240.55	47199.29	6115.93
58251.02	33534.35	-11596.65
68134.73	19073.32	-30147.73

Using the TDOA measurements d_{ij} in Table 3, a set of three hyperboloids is computed from Equation (5) at each of the 10 time instants. Target location are then extracted by finding the intersection point of the three hyperboloid surfaces at each of the 10 time instants to generate a target track. Details of the target localization process are discussed in Section 4 of [1].

To assess the accuracy of TDOA processing over the Earth's curved surface, the target locations obtained in (x,y,z) frame are transformed back to the world geodetic coordinate frame $(\text{lat},\text{lon},\text{alt})$; this is a reversed procedure going from the bottom stage in Figure 14 back to the top. In this reversed transforming direction, (x,y,z) is first converted back to the local geodetic frame $(N,E,U) = (x,y,z)$ through a series of 3 reversed frame rotations, $-\gamma$, $-\beta$ and $-\theta$, where θ , β , γ are given by Equations (11), (13) and (15) respectively. This is then followed by a switch of the tangential plane axes back to the local geodetic frame,

$$\begin{aligned} x &= y' \text{ (North)} \\ y &= x' \text{ (East)} \\ z &= z' \text{ (Up)} \end{aligned} \quad (20)$$

Then a transformation from the local geodetic frame (N,E,U) is converted to the conventional terrestrial frame (X,Y,Z) via [9,10,12],

$$\begin{pmatrix} X \\ Y \\ Z \end{pmatrix} = \begin{pmatrix} X_0 \\ Y_0 \\ Z_0 \end{pmatrix} + \begin{pmatrix} -\sin \phi \cos \lambda & -\sin \lambda & \cos \phi \cos \lambda \\ -\sin \phi \sin \lambda & \cos \lambda & \cos \phi \sin \lambda \\ \cos \phi & 0 & \sin \phi \end{pmatrix} \begin{pmatrix} x \\ y \\ z \end{pmatrix} \quad (21)$$

As the final step, (X,Y,Z) is converted back to the world geodetic coordinates (ϕ,λ,h) (i.e., $(\text{lat},\text{lon},\text{alt})$) [p.100, 9],

$$\begin{aligned} \phi &= \tan^{-1} \left(\frac{Z}{\sqrt{X^2 + Y^2}} \left(1 - e^2 \frac{N}{N+h} \right)^{-1} \right) \\ \lambda &= \tan^{-1} \left(\frac{Y}{X} \right) \\ h &= \frac{\sqrt{X^2 + Y^2}}{\cos \phi} \end{aligned} \quad (22)$$

where e and N are given in Equation (6). The quantities ϕ and h in Equation (22) can be solved only by iterative methods. Closed formulas with negligible residual error have been developed by [19] known as the ‘‘Bowring formulas,’’ and the algorithm for computing Equation 22 is available as a standard geodetic algorithm in [10].

4.3 Target localization results

The target's actual track (ground truth) is mapped from the world geodetic coordinates (lat,lon,alt) to the Cartesian coordinates (x,y,z) through the flow diagram as shown in Figure 14. The target's ground-truths in (x,y) are shown by the open black circles in Figure 17. The TDOA measurements d_{ij} taken from the target track (Table 3) are input into the target localization process using the geometric approach described in [1].

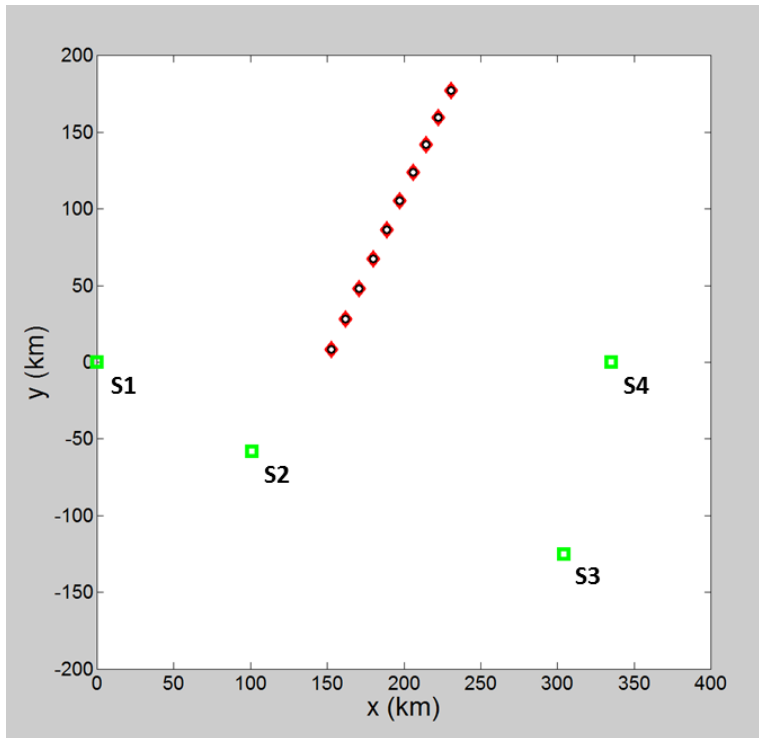


Figure 17: Target localization results from TDOA measurements. Open black circles = ground truth; red diamonds = computed target locations.

The computed target locations at the 10 time instants are plotted in Figure 17 as red diamonds. It can be seen graphically that the computed target locations are in excellent agreement with the target ground truth. The numerical results are tabulated in Table 4. First, it is noted that the target's ground truths vary in height z_g in the global Cartesian frame, even though it is cruising at a constant altitude in the world geodetic coordinate frame. This is a consequence of the curvature of Earth as explained in Section 1. As the target is far away from the receiver system, it appears lower towards the horizon in the global Cartesian frame. As the target approaches closer to the receiver system, it rises higher in height. This is consistent with what is observed in a real-world scenario of a target approaching from afar. In Table 4, the target's height in the global Cartesian frame appears to be greater than the target's altitude of 16000 m. This is due to the tilting of the conventionalized geodetic frame to the final global Cartesian frame through a series of three rotating transformation as indicated in Figures 11, 12 and 13 (i.e., the last three stages in Figure 14).

Table 4: Results of target localization in the global Cartesian coordinate frame (x,y,z).

Target ground truths (m)			Computed target locations (m)		
x_g	y_g	z_g	x	y	z
230597.25	177313.23	14745.02	230595.46	177309.73	14700.00
222475.43	159741.80	15350.39	222477.27	159745.26	15400.00
214222.20	141885.57	15905.59	214222.01	141885.23	15900.00
205834.39	123737.65	16407.93	205834.15	123737.25	16400.00
197308.75	105290.96	16854.57	197310.00	105292.76	16900.00
188641.90	86538.21	17242.53	188640.85	86537.03	17200.00
179830.40	67471.86	17568.67	179831.11	67472.32	17600.00
170870.66	48084.18	17829.69	170870.01	48084.19	17800.00
161759.03	28367.19	18022.12	161758.48	28367.58	18000.00
152491.70	8312.65	18142.32	152490.24	8314.36	18100.00

From Table 4, it is seen that the computed target locations (x,y,z) are in very close agreement with the target's ground-truth values (x_g, y_g, z_g). The difference between the two is less than 4 m in x and y. This slight discrepancy is due to the fact that the computed target positions (x,y) are determined by scanning the height z of the three intersecting hyperboloids in 100 m increments. Thus, the computed target's height is never matched to that of the target's ground truth; therefore, the computed x and y values do not match exactly to the ground truth values. An error of less than 4 m in the target position (x,y) is not a major issue in most applications in determining the location of a large target, for example, an aircraft. Real-time target localization is more of a concern and challenge in practical surveillance applications in which the threat must be identified and dealt with immediately. The time taken to compute a target location at one time sample in this work is around 63 s. The amount of time required is proportional to the size of the surveillance area because the size of the hyperboloids has to be big enough to cover the surveillance area. A computation time of less than 1 s per time instant is sought for real-time application.

In presenting target location information to human operators and analysts, the computed target locations in (x,y,z) shown in Figure 17 have to be converted to world geodetic coordinates; i.e., (lat,lon,alt). These can then be displayed on a geographic map such as Google Earth to present a clear familiar picture to the human operators. This is achieved by transforming (x,y,z) through a reversed conversion operation back to (lat,lon,alt) as described in Section 4.2; this reversed conversion process is shown in Figure 14, going from bottom stage back to the top stage in the flow diagram.

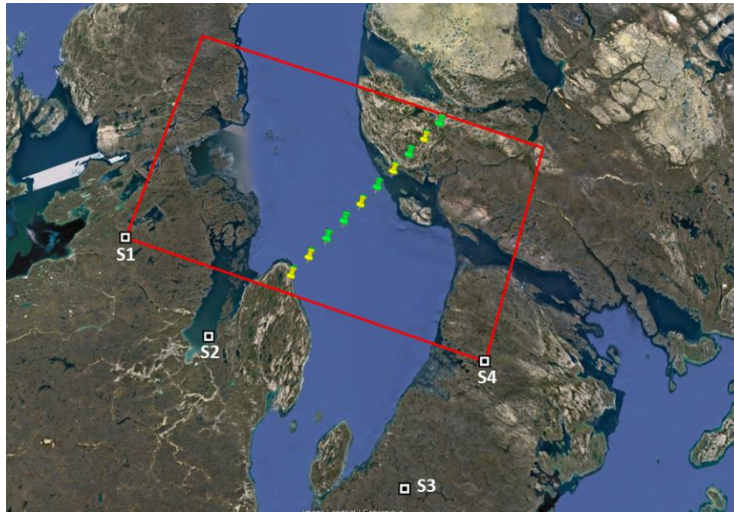


Figure 18: Target locations displayed on Google Earth map. Yellow = ground truths. Green = computed.

Results of the target locations converted back to the world geodetic coordinates are shown in Figure 18. It can be seen that the computed target locations are overlapping the target's ground-truth very precisely. A numerical comparison between the two is given in Table 5. The computed altitude and latitude are almost exactly the same as the ground truth values. While the target's ground-truth altitude is constant at 16000 m, the computed altitude varies slightly about the ground truth values by less than 50 m. This is again due to the computed altitude being based on an incremental scan of 100 m along the height direction in the TDOA processing.

Table 5: Results of target localization in the world geodetic coordinate frame (lat,lon,alt).

Target ground truths			Computed target locations		
lat _g (deg)	lon _g (deg)	alt _g (m)	lat (deg)	lon (deg)	alt (m)
70.6860	-87.1230	16000	70.6860	-87.1231	15954.88
70.5253	-87.3171	16000	70.5253	-87.3170	16049.70
70.3618	-87.5111	16000	70.3618	-87.5111	15994.40
70.1954	-87.7051	16000	70.1954	-87.7051	15992.06
70.0261	-87.8991	16000	70.0261	-87.8991	16045.46
69.8538	-88.0931	16000	69.8538	-88.0932	15957.45
69.6784	-88.2872	16000	69.6784	-88.2871	16031.34
69.4998	-88.4812	16000	69.4998	-88.4812	15970.31
69.3180	-88.6752	16000	69.3180	-88.6752	15977.88
69.1328	-88.8692	16000	69.1328	-88.8693	15957.69

5 Conclusions

An investigation of TDOA processing for geo-locating a target within a large surveillance area over a curved surface of the Earth is presented. A three-dimensional target localization procedure is carried out in a Cartesian coordinate frame permitting a simpler computational model of the TDOA equations as given in Equation 1 to be used instead of a more complex ellipsoidal coordinate frame model using curvilinear coordinates (latitude, longitude). Furthermore, the Cartesian frame model enables a geometric approach to solving the target localization problem.

The geometric approach enables TDOA processing using data collected from a detection system deploying the minimum number of receivers. This minimum number is four for three-dimensional geolocation processing.

A scenario is described in this study on how to localize a target in a large surveillance area with the effect of the Earth's surface curvature taken into consideration. The Earth's surface curvature introduces a curved target flight path with varying height in a Cartesian coordinate frame. The separation distance between a pair of receivers that is used to make the TDOA measurement must be described in terms of a line-of-sight chord length instead of an arc length along the surface of the Earth. To accommodate these adjustments in solving the target localization problem via the TDOA equations given in Equation (1), a procedure has been developed to transform a curved surface in the world geodetic coordinate frame (lat,lon,alt) to a global Cartesian coordinate frame (x,y,z). A 4-receiver non-coplanar detection system configuration is used in the TDOA processing analysis. The computed results have shown that the procedure of transforming the curved world geodetic coordinates to Cartesian coordinates can facilitate proper target localization over a curved segment of the Earth's surface.

TDOA processing over a large surveillance area offers some practical applications. In remote regions of the Earth, such as in the Arctic, accessing and servicing of receiver installations are challenging issues in terms of logistics and cost. Thus it is desirable to minimize the number of receivers used to make the surveillance operation economically viable over a long period. Moreover, more receivers mean a larger volume of data will need to be collected and the data will have to be transmitted to a central data centre for processing. This will require substantially greater data link capacity to support the surveillance activity, requiring additional supporting resources. In addition, more computational resources are also needed to handle the larger volume of data that has to be processed and analyzed. Thus, minimizing the number of receivers deployed over a given area of interest will significantly reduce the complexity of the overall target detection and tracking operation.

References

- [1] S. Wong, R. Jassemi-Zargani, D. Brookes and B. Kim, “Passive target localization using a geometric approach to the time-difference-of-arrival method,” Scientific Report, DRDC-RDDC-2017-R079, Defence Research and Development Canada, June 2017.
- [2] ”The Methodology for Assessing Technology Triggered Threats (MAT3),” RCAF/DRDC war-game exercise, Canadian Forces Aerospace Warfare Centre, Trenton Air Force Base, April 24–25, 2013.
- [3] ”NASA Wants to Fly Drones on Mars to Look For Natural Resources,” J. Zhou, *Epoch Times*, August 5, 2015. <http://www.theepochtimes.com/n3/1706045-nasa-wants-to-fly-drones-on-mars/> (accessed January 2017).
- [4] “Geometric distance to horizon,” https://en.wikiipedia.org/wiki/Line-of-sight_propagation (accessed November 2016).
- [5] “Class 2, Mode S transponders,” <https://www.cumulus-soaring.com/transponders.htm> (accessed November 2016).
- [6] J. P. Van Etten, “Navigation Systems: Fundamentals of Low- and Very-Low-Frequency Hyperbolic Techniques,” *Electrical Communication*, Vol. 45, No. 3, pp.192–212, 1970.
- [7] H. C. Schau and A. Z. Robinson, “Passive Sources Localization Employing Intersecting Spherical Surfaces from Time-of-Arrival Differences,” *IEEE Transactions on Acoustics, Speech, and Signal Processing*, Vol. ASSP-35, No.8 pp.1223–1225, August 1987.
- [8] D. A. Brannan, M. F. Esplen and J. J. Grey, *Geometry*, Cambridge University Press, 1999.
- [9] W. Torge, *Geodesy*, Third Edition, Walter de Gruyer, New York, 2001.
- [10] MATLAB KML Geodetic Toolbox, M. R. Craymer, 2011.
- [11] “Geodetic and geocentric latitudes,” <https://en.wikipedia.org/wiki/latitude> (accessed November 2016).
- [12] R. Chen and R. E. Guinness, *Geospatial Computing in Mobile Devices*, Artech House, Boston, 2014.
- [13] “Geographic coordinate conversion – Geodetic to/from ENU coordinates,” https://en.wikipedia.org/wiki/Geographic_coordinate_conversion (accessed April 2017).
- [14] H. Flanders, R. Korfhage, J. Price, *A Second Course in Calculus*, Academic Press, New York, 1974.
- [15] W. Stutzman and G. Thide, *Antenna Theory and Design*, John Wiley & Sons, Inc. p. 60 1981.
- [16] ”Automatic Dependent Surveillance–Broadcast,” www.avionicswest.com/Articles/ADSB.html (accessed January 2017).

- [17] "Communications Satellite Constellations, MIT Industry Systems Study," http://ardent.mit.edu/real_options/de%20Week%System%20Study/unit1_summary.pdf (accessed June 2014).
- [18] "Iridium Subscriber License Information. Rev1.26b 09 February 2013," http://marine.rutgers.edu/~kerfoot/pub/slocum/RELEASE_6_32/src/doco/specifications/iridium-phone/IR_Lband.doc.rtf (accessed June 2014).
- [19] B. R. Bowring, "The accuracy of geodetic latitude and height equations," Survey Review 28, pp. 202–206, 1985.

List of symbols/abbreviations/acronyms/initialisms

ADB-S	Automatic Dependent Surveillance-Broadcast
CAF	Canadian Armed Forces
EIRP	Effective Isotropic Radiated Power
IFF	Identification Friend or Foe
ISR	Intelligence, Surveillance and Reconnaissance
LOS	Line-Of-Sight
RF	Radio-Frequency
SNR	Signal-to-Noise Ratio
TDOA	Time-Difference-Of-Arrival

DOCUMENT CONTROL DATA

*Security markings for the title, authors, abstract and keywords must be entered when the document is sensitive

1. ORIGINATOR (Name and address of the organization preparing the document. A DRDC Centre sponsoring a contractor's report, or tasking agency, is entered in Section 8.) DRDC – Ottawa Research Centre Defence Research and Development Canada 3701 Carling Avenue Ottawa, Ontario K1A 0Z4 Canada		2a. SECURITY MARKING (Overall security marking of the document including special supplemental markings if applicable.) CAN UNCLASSIFIED
		2b. CONTROLLED GOODS NON-CONTROLLED GOODS DMC A
3. TITLE (The document title and sub-title as indicated on the title page.) Target localization over the Earth's curved surface		
4. AUTHORS (Last name, followed by initials – ranks, titles, etc., not to be used) , S. W.; Kaluzny, B.		
5. DATE OF PUBLICATION (Month and year of publication of document.) May 2018	6a. NO. OF PAGES (Total pages, including Annexes, excluding DCD, covering and verso pages.) 34	6b. NO. OF REFS (Total references cited.) 19
7. DOCUMENT CATEGORY (e.g., Scientific Report, Contract Report, Scientific Letter.) Scientific Report		
8. SPONSORING CENTRE (The name and address of the department project office or laboratory sponsoring the research and development.) DRDC – Ottawa Research Centre Defence Research and Development Canada 3701 Carling Avenue Ottawa, Ontario K1A 0Z4 Canada		
9a. PROJECT OR GRANT NO. (If appropriate, the applicable research and development project or grant number under which the document was written. Please specify whether project or grant.)	9b. CONTRACT NO. (If appropriate, the applicable number under which the document was written.)	
10a. DRDC PUBLICATION NUMBER (The official document number by which the document is identified by the originating activity. This number must be unique to this document.) DRDC-RDDC-2018-R136	10b. OTHER DOCUMENT NO(s). (Any other numbers which may be assigned this document either by the originator or by the sponsor.)	
11a. FUTURE DISTRIBUTION WITHIN CANADA (Approval for further dissemination of the document. Security classification must also be considered.) Public release		
11b. FUTURE DISTRIBUTION OUTSIDE CANADA (Approval for further dissemination of the document. Security classification must also be considered.)		
12. KEYWORDS, DESCRIPTORS or IDENTIFIERS (Use semi-colon as a delimiter.) Intelligence; Surveillance and Reconnaissance; signal processing; counter-measures; passive detection and tracking; target localization; wide-area air surveillance; large areas situational awareness		

A procedure has been developed to enable target geolocation information to be processed from data collected over a wide surveillance area in which the effect of the Earth's surface curvature is notable. The surveillance area of interest on the curved surface and its associated air space are transformed from the ellipsoidal (world geodetic) frame with coordinates given in latitude, longitude and altitude to an appropriate Cartesian frame with coordinates given by x , y , z . The Cartesian coordinate system permits a simpler three-dimensional model for processing of the target's locations. It also allows a geometric approach to be used to solve the TDOA equations, using hyperboloids as solutions to the TDOA problem. The appeal of the geometric approach is its applicability in target geolocation processing using data collected from a minimum number of receivers deployed in a passive detection system as discussed in a previous study in [1].

Results have shown that the TDOA processing procedure developed in this study can provide proper target localization over a curved segment of the Earth's surface. TDOA processing over a wide surveillance area is desirable in a practical passive detection system. It enables a reduction in the overall detection system's physical complexity by reducing the minimum number of receivers deployed, thereby reducing the amount of data to be collected and processed.

On a élaboré une procédure permettant le traitement de données de géolocalisation de cibles à partir des données de surveillance recueillies au-dessus d'un vaste territoire où l'effet de l'incurvation de la surface terrestre est perceptible. La zone de surveillance d'intérêt sur la surface incurvée et son espace aérien connexe est transformée d'un cadre ellipsoïdal (géodésique mondial) avec coordonnées exprimées en latitude, longitude et altitude en un cadre cartésien avec coordonnées exprimées en x , y , z . Le système de coordonnées cartésiennes constitue un modèle tridimensionnel simplifié pour le traitement de l'emplacement des cibles. Il permet également l'utilisation d'une approche géométrique pour la résolution des équations TDOA. Il permet notamment l'utilisation d'hyperboloïdes comme solutions au problème de TDOA. L'avantage de l'approche géométrique réside dans la possibilité de l'utiliser pour la géolocalisation de cibles à partir de données recueillies par un nombre minimal de récepteurs déployés dans un réseau de détection passif, tel qu'abordé dans une étude antérieure [1].

Les résultats ont démontré que la procédure de traitement TDOA élaborée dans le cadre de cette étude permet de localiser efficacement une cible au-dessus d'un segment incurvé de la surface terrestre. Le traitement TDOA appliqué à une vaste zone de surveillance est souhaitable dans un système de détection passif. Il permet la réduction de la complexité physique du système de détection global en réduisant le nombre de récepteurs déployés, ce qui réduit la quantité de données à colliger et à traiter.